Journal of Experimental Botany, Vol. 62, No. 3, pp. 1271–1284, 2011
doi:10.1093/jxb/erq363 Advance Access publication 13 December, 2010
This paper is available online free of all access charges (see http://jxb.oxfordjournals.org/open_access.html for further details)

Journal of Experimental Botany
www.jxb.oxfordjournals.org

RESEARCH PAPER

RCD1 and *SRO1* are necessary to maintain meristematic fate in *Arabidopsis thaliana*

Sachin Teotia[1,†] and Rebecca S. Lamb[1,2,*]

[1] Molecular, Cellular and Developmental Biology Program, The Ohio State University, 500 Aronoff Laboratory, 318 W. 12th Ave, Columbus OH 43210, USA

[2] Plant Cellular and Molecular Biology Department, The Ohio State University, 500 Aronoff Laboratory, 318 W. 12th Ave, Columbus, OH 43210, USA

[†] Current address: School of Biotechnology, Gautam Buddha University, Greater Noida, 201308, India

* To whom correspondence should be addressed: E-mail: lamb.129@osu.edu

Abstract

The *RADICAL-INDUCED CELL DEATH1* and *SIMILAR TO RCD ONE1* genes of *Arabidopsis thaliana* encode members of the poly(ADP-ribose) polymerase (PARP) superfamily and have pleiotropic functions in development and abiotic stress response. In order to begin to understand the developmental and molecular bases of the defects seen in *rcd1-3; sro1-1* plants, this study used the root as a model. Double mutant roots are short and display abnormally organized root apical meristems. However, acquisition of most cell fates within the root is not significantly disrupted. The identity of the quiescent centre is compromised, the zone of cell division is smaller than in wild-type roots and abnormal divisions are common, suggesting that *RCD1* and *SRO1* are necessary to maintain cells in a division-competent state and to regulate division plane placement. In addition, differentiation of several cell types is disrupted in *rcd1-3; sro1-1* roots and shoots, demonstrating that *RCD1* and *SRO1* are also necessary for proper cell differentiation. Based on the data shown in this article and previous work, we hypothesize that RCD1 and SRO1 are involved in redox control and, in their absence, an altered redox balance leads to abnormal development.

Key words: Cell division, meristems, PARP, RCD1, redox balance, root development, SRO1.

Introduction

In plants, most morphogenesis takes place post-embryonically through the action of two distally localized groups of stem cells, the shoot apical meristem (SAM) and the root apical meristem (RAM). These meristems are established during embryogenesis and maintained throughout the life of the plant. The SAM is responsible for the generation of the stem, leaves, and inflorescence of the plant while the RAM makes the root. The number of stem cells within the meristems is maintained by a balance between cell division and cell differentiation. The RAM consists of initial cells in a single layer surrounding the quiescent centre (QC), thought to be the organizing cells (van den Berg *et al.*, 1997). Maintenance of the pluripotent identity of the RAM cells is controlled by SHORTROOT/SCARECROW (SHR/SCR) and the auxin-dependent expression of the *PLETHORA* (*PLT*) genes (Sabatini *et al.*, 1999, 2003; Aida *et al.*, 2004) and the homeobox transcription factor WOX5 (Stahl *et al.*, 2009). In addition to these pathways, it is known that redox components within the RAM are also important for its maintenance and function (reviewed in De Tullio *et al.*, 2010).

The poly(ADP-ribose) polymerase (PARP) superfamily is composed of proteins containing the PARP catalytic site, also known as the PARP signature. Members of this family include enzymes that modify target proteins by attaching ADP-ribose subunits from NAD^+ post-translationally to

Abbreviations: BA, 6-benzylaminopurine; DAPI, 4',6-diamidino-2-phenylindole; GFP, green fluorescent protein; GSH, glutathione; GUS, β-glucuronidase; NAA, 1-naphthaleneacetic acid; QC, quiescent centre; RAM, root apical meristem; ROS, reactive oxygen species; RST, RCD–SRO–TAF4 domain; SAM, shoot apical meristem; SIMR, stress-induced morphological response.

target proteins. These units can be added as chains by genuine PARPs or as single ADP-ribose moieties by a subset of PARP-like proteins termed mono(ADP-ribose) transferases (mARTs). In addition, some PARP superfamily members do not apparently function as enzymes (reviewed in Hassa and Hottiger, 2008; Hottiger *et al.*, 2010). Orthologues of the so-called 'classical PARPs' from animals, known to function in DNA repair, have been identified in plants (Lepiniec *et al.*, 1995; Babiychuk *et al.*, 1998). In the model plant species *Arabidopsis thaliana*, they appear to function in DNA repair, stress response, and response to pathogens (Amor *et al.*, 1998; Doucet-Chabeaud *et al.*, 2001; De Block *et al.*, 2005; Vanderauwera *et al.*, 2007; Foyer *et al.*, 2008; Pellny *et al.*, 2009; Adams-Phillips *et al.*, 2008, 2010). In addition to these proteins, the Embryophyta (land plants) encode members of a unique clade of PARP-like proteins (Citarelli *et al.*, 2010; Jaspers *et al.*, 2010). This clade contains proteins with an RST (RCD–SRO–TAF4) domain C-terminal to their PARP signature and a subset of the proteins are also characterized by a WWE protein–protein interaction domain in their N-termini (Citarelli *et al.*, 2010; Jaspers *et al.*, 2010). Arabidopsis encodes two paralogous genes, *RADICAL-INDUCED CELL DEATH1* (*RCD1*) and *SIMILAR TO RCD ONE 1* (*SRO1*), which are members of the WWE-containing subclade (Belles-Boix *et al.*, 2000; Ahlfors *et al.*, 2004). These genes have pleiotropic roles during both stress response and development and are partially redundant with one another (Jaspers *et al.*, 2009; Teotia and Lamb, 2009). Double mutants in both *RCD1* and *SRO1* have severe developmental defects. Most *rcd1-3; sro1-1* individuals do not survive embryogenesis and die with defects in the SAM, RAM, and hypocotyl, demonstrating that the function(s) encoded by these genes are critical for plants (Teotia and Lamb, 2009). Those that do survive have pleiotropic phenotypes including short stature, short roots, and reduced apical dominance (Jaspers *et al.*, 2009; Teotia and Lamb, 2009).

RCD1 does not appear to have PARP or mART enzymatic function (Jaspers *et al.*, 2010); this has not been assayed for SRO1. Therefore, the molecular function of these proteins is unclear. However, they are known to bind to transcription factors (Belles-Boix *et al.*, 2000; Ahlfors *et al.*, 2004; Jaspers *et al.*, 2009), suggesting that they are involved in transcriptional regulation. *rcd1* mutants accumulate both reactive oxygen species (ROS) (Overmyer *et al.*, 2000) and nitric oxide (Ahlfors *et al.*, 2008), even under normal growth conditions, suggesting that it negatively regulates the accumulation of these compounds, directly or indirectly. In addition, the expression of genes known to indicate oxidative stress, *AOX1a* and *UPOX*, is constitutively upregulated in *rcd1-3* mutants (Jaspers *et al.*, 2009). *rcd1-3; sro1-1* double mutants appear to be under constitutive stress, as indicated by accumulation of excess sumoylated proteins and an increase in the expression of the stress-inducible gene *PARP2*. Many of the phenotypic defects seen in *rcd1-3; sro1-1* are similar to those seen in the stress-induced morphological response (SIMR) (Teotia *et al.*, 2010), known to be associated with changes in redox balance (Potters *et al.*, 2009). Therefore, an important function of these genes is to regulate the redox environment within the cell.

In this study we investigated the role of *RCD1* and *SRO1* in cell division and differentiation using the root as a model system. We demonstrate that these genes are necessary to maintain proper cell division in the RAM of Arabidopsis and for proper differentiation of several cell types, including xylem vessels and fibres, and root cap cells.

Materials and methods

Plant materials and growth conditions

Arabidopsis seeds were vernalized for 3–5 days and grown on Fafard-2 Mix soil with sub-irrigation at 22 °C with 50% relative humidity under long-day irradiance (16 h, 80 μmol m^{-2} s^{-1}) in controlled growth chambers (Enconair Ecological Chambers). Seeds used for marker line analysis were sterilized with 70% ethanol followed by 40% (v/v) hypochlorite (bleach) and placed on Murashige and Skoog (MS) medium (RPI) agar plates containing 1% sucrose, incubated in the dark for 3 days at 4 °C, and then grown vertically. Seedlings used for root growth assays were sown on half-MS and 1% sucrose media and grown vertically. Plants for the marker line analysis were grown on plates vertically for 7–10 days. All seedlings grown on plates were grown under long-day conditions at 22 °C in a Plant Growth Chamber (Percival Scientific).

rcd1-3, sro1-1 and *rcd1-3; sro1-1* mutants have been described previously (Teotia and Lamb, 2009). Marker lines used are listed in Table S1 (Supplementary data are available at *JXB* online). In order to introduce marker transgenes into the *rcd1-3; sro1-1* background, *rcd1-3; sro1-1* plants were crossed to the marker lines, the F1 plants allowed to self, and F2 seeds were analysed for expression.

Phenotypic analysis of mutants

Root phenotypes were analysed in the wild type (Columbia), *rcd1-3*, *sro1-1* and *rcd1-3; sro1-1* plants. For root length analysis at least 25 plants of each genotype were analysed in two independent replicates. Measurement of the root division zone was done using at least 15 plants of each genotype and this region was defined as the area from the QC to the start of the elongation zone. The number of root meristematic cells was obtained by counting the cortical cells showing no signs of rapid elongation in the above-defined division zone. The ability of plants to respond to cytokinin and auxin was determined by growing seedlings vertically for 5 days and then transferring seedlings to mock or hormone-containing media, growing for a further 4 days, and then measuring the growth of the root while on the media. The cytokinin 6-benzylaminopurine (BA; PhytoTechnology Laboratories) was used at concentrations of 0.01, 0.1, 1, and 10 μM. The auxin 1-naphthaleneacetic acid (NAA; PhytoTechnology Laboratories) was used at concentrations of 1, 20, 40, 60, 80, and 100 nM. The number of flowers produced by wild-type and *rcd1-3; sro1-1* plants was determined for 25 plants of each genotype. Only flowers produced on the primary inflorescence were counted. Retention of lateral root cap cells in wild-type and double mutant roots was analysed by examination of primary roots under a Nikon SMZ800 dissecting microscope and defined as the presence of lateral root cap cells attached to the epidermis at least five cell lengths into the elongation zone. Wherever indicated in the text, significant difference between the phenotypes of the mutants and the wild type was calculated, at $P < 0.01$, by Student's t test.

For analysis of marker gene expression in the *rcd1-3; sro1-1* background, F2 seeds of each cross were plated and expression

was compared between the double mutants and the siblings whose phenotype resembled wild type (referred to as WT-like in the text) growing on the same plate. *rcd1-3; sro1-1* seedlings were easily identified on the basis of their distinct phenotype (Teotia and Lamb, 2009). In case of *DR5rev::GFP* expression, *rcd1-3; sro1-1* from F3 or F4 generations were compared with the wild type. For each line at least 30–35 individuals of the double mutants and 40–50 individuals of WT-like plants were analysed for expression in each of two biological replicates.

Visualization of β-glucuronidase expression

Seedlings 7–10 days old were used to examine expression of β-glucuronidase (GUS) driven in marker lines. Seedlings were incubated in 90% acetone for 30 min on ice and washed twice with 100 mM sodium phosphate buffer (pH 7). The tissues were then incubated in GUS staining buffer (100 mM sodium phosphate buffer pH 7, 1 mM potassium ferricyanide, 1 mM potassium ferrocyanide, 0.1% Triton X-100, 10 mM EDTA, 1–1.5 mM 5-bromo-4-chloro-3-indolyl-β-D-glucuronic acid) at 37 °C for various lengths of time depending on the strength of expression. Seedlings were then washed and stored in 70% ethanol. Photographs were taken by a Nikon Digital Sight DS-5M camera on a Nikon SMZ800 dissecting or on a Nikon Eclipse E200 compound microscope.

Histology and microscopy

Leaves and stems from at least five independent adult plants were cut into small pieces and then fixed in 3% (v/v) glutaraldehyde + 2% (v/v) paraformaldehyde [Electron Microscopy Sciences (EMS), Hatfield, PA, USA] in 0.1 M phosphate buffer pH 7.2 by vacuum infiltration and then overnight at 4 °C. Fixed samples were washed once for 15 min with 0.1 M potassium phosphate buffer pH 7.2 and then four times with distilled water. Samples were then dehydrated through an ethanol series 25, 50, 70, 90, and 100% (four times), each step for 15 min at room temperature. Samples were then put in resin for resin infiltration with the following steps: 2 parts 100% ethanol + 1 part Spurr's resin (EMS; 1 h); 1 part 100% ethanol + 1 part Spurr's resin (2 h); 1 part 100% ethanol + 3 parts Spurr's resin (2 h); 100% Spurr's resin (1 h); 100% Spurr's resin overnight. The next day the tissues along with the resin were put in moulds (EMS) with the desired orientation and left at 65 °C for 36 h to solidify. Roots were fixed in the same manner as described above, except the dehydration series was continued to 90% alcohol. Infiltration was done with 100% LR white resin (EMS) for 2 h at room temperature and then tissues were embedded in capsules with LR white resin for 24 h at 55 °C. The leaves and stem sections were cut with ultramicrotome [Reichert-Jung (Leica) Ultra-cut 701701] at 2 μm thickness and sections were stained for 2 min with 1% toluidene blue (1 g toluidene blue, 1 g sodium borate, and 100 ml of water). Root sections (1 μm) were cut with a Leica Ultracut UCT ultramicrotome and stained with 1% safranin. The sections were mounted permanently on slides with Permount (Fischer).

Hand-sections of 7- to 10-day-old roots were obtained as described (Benfey *et al.*, 1993). The sections were placed in water on a slide, stained with fluorescent brightener-28 (Sigma) and observed by epifluorescence microscopy using a Nikon Eclipse 90i microscope equipped with Nikon Intensilight C-HGFI Fiber Illuminator.

In order to visualize nuclear size in root cells, 6-day-old roots were fixed in PEMT buffer as described (Sugimoto *et al.*, 2000). Fixed seedlings were washed three times with PEMT buffer for 10 min each followed by three washes with phosphate-buffered saline. Roots were dissected from the seedlings and mounted in Vectashield mounting medium (Vector Laboratories) with 1.5 μg/ml 4',6-diamidino-2-phenylindole (DAPI). UV epifluorescence microscopy observations were performed using a Nikon Eclipse 90i microscope.

For confocal laser imaging of roots, cell walls were labelled with propidium iodide as described (Truernit *et al.*, 2008). Roots were observed by Nikon D-Eclipse C1si Confocal microscope using the excitation wavelength of 488 nm, and emission was collected at 620–720 nm. Marker lines where green fluorescent protein (GFP) was the marker were observed using laser confocal microscopy as above using an excitation wavelength of 488–562 nm.

Starch granules in the columella root cap were visualized in 5-day-old seedlings, grown on half-MS plates, as described by Willemsen *et al.* (1998). Seedlings were stained for 2 min, rinsed with water, and cleared with chloral hydrate. All sections and starch granules in roots were observed under a Nikon Eclipse E200 compound microscope equipped with the Nikon Digital Sight DS-5M camera. All images were put into equal-sized canvases of the same resolution to make a composite figure with Adobe Photoshop version 7.0.

Results

RCD1 *and* SRO1 *have dynamic expression patterns*

RCD1 and *SRO1* are expressed in all organs of the plant (Jaspers *et al.*, 2009; Teotia and Lamb, 2009), with higher expression found in the vascular tissues in particular

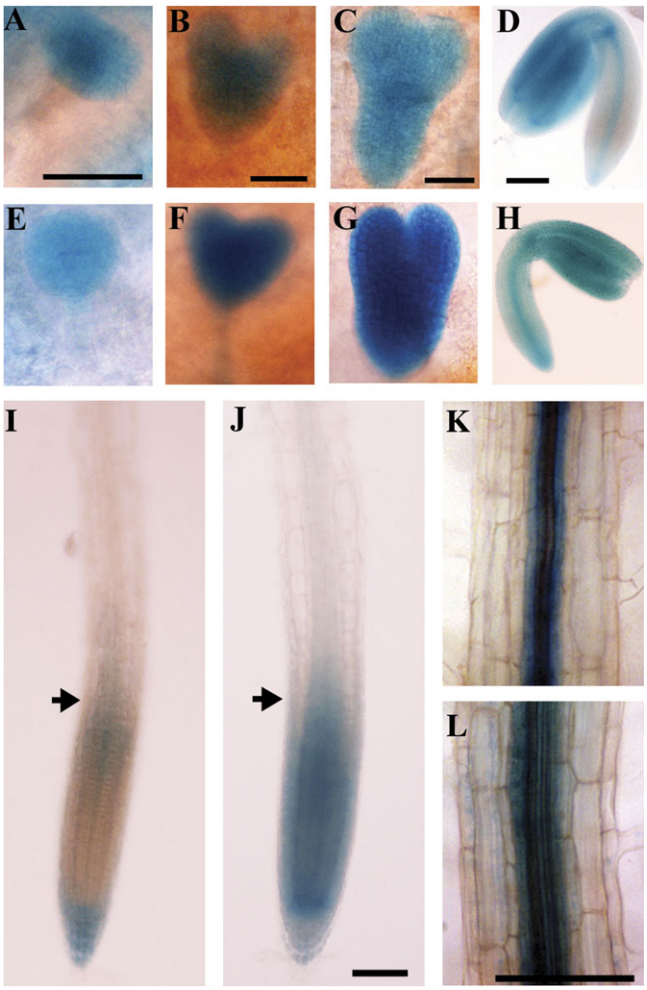

Fig. 1. *RCD1* and *SRO1* are expressed throughout the embryo and in the root meristem. Staining for GUS activity in embryos and roots of *RCD1::GUS* (A–D, I, K) and *SRO1::GUS* (E–H, J, L) are shown. Arrows indicate end of division zone in (I, J). Scale bars represent 100 μm.

(Jaspers *et al.*, 2009). Expression begins at the globular stage of embryogenesis, when both genes are expressed throughout the embryo proper but not in the suspensor (Fig. 1A, E). Expression continues throughout the embryo until the torpedo stage (Fig. 1B, C, F, G), after which expression within the procambial strands becomes pronounced (Fig. 1D, H). This pattern is consistent with publically available microarray data (Winter *et al.*, 2007). Postembryonically, both *RCD1* and *SRO1* are expressed in the root tips (Fig. 1I, J); however, while *RCD1* expression is most prominent in the region of the QC and root cap (Fig. 1I), *SRO1* is strongly expressed throughout the division zone of the root (Fig. 1J). Both genes are also expressed in the differentiating vascular cells of the root (Fig. 1K, L; Jaspers *et al.*, 2009). In addition, examination of publically available microarray data suggests that low levels of expression are found in most cells of the plant, with the exception of the trichomes, and pavement cells of the leaves (Winter *et al.*, 2007).

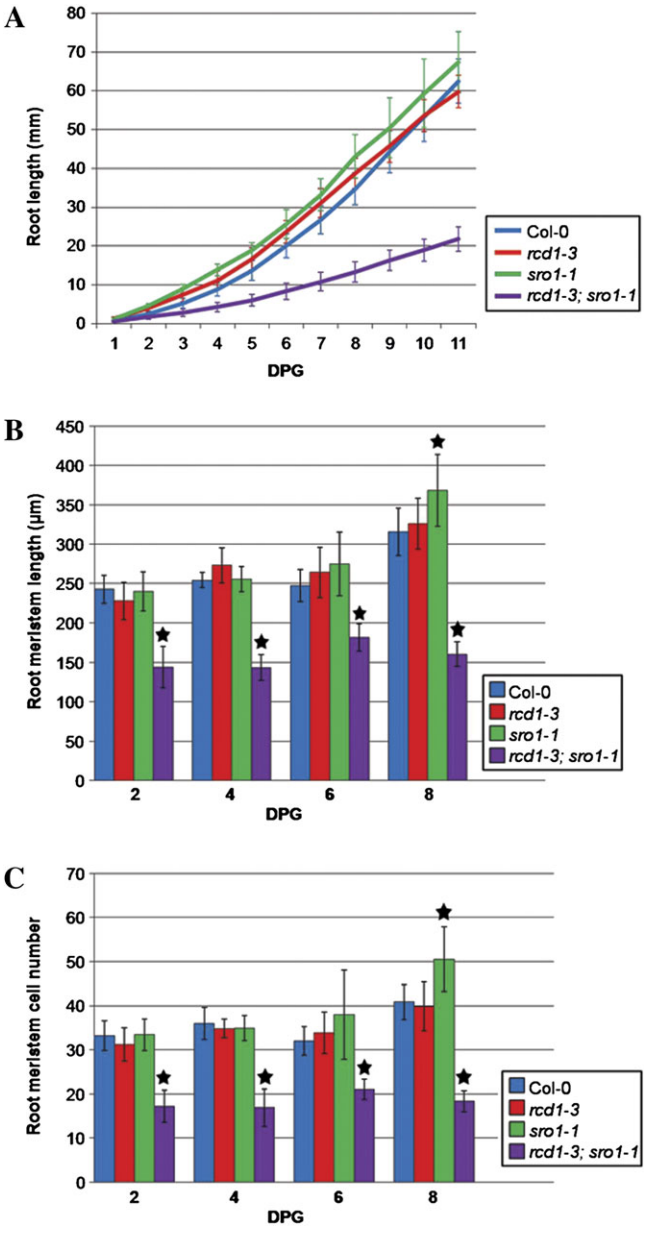

Fig. 2. Root length and meristem size are reduced in *rcd1-3; sro1-1* plants. (A) Root growth curves. (B) Root meristem length. (C) Root meristem cell number. Stars indicate values significantly different from the wild type at $P < 0.01$. Error bars indicate standard deviation. Col-0, Columbia; DPG, days post-germination.

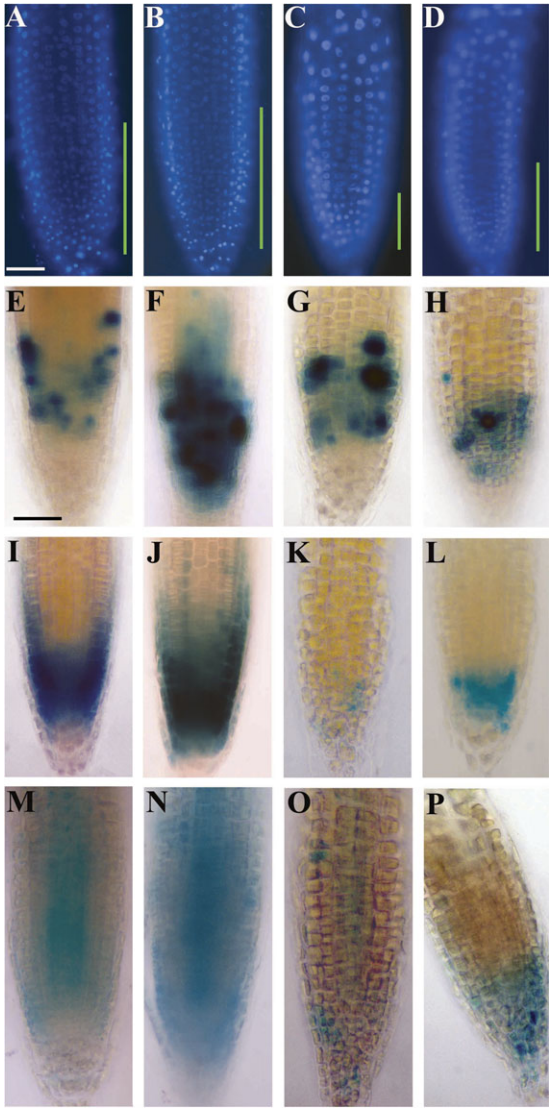

Fig. 3. *RCD1* and *SRO1* control proliferation in the root tip. (A–D) DAPI-stained roots: Col-0 (A, B), *rcd1-3; sro1-1* (C, D). (E–H) Staining for GUS activity of *CYCB1; 1::GUS* for 4 h in the root tip: WT-like (E, F), *rcd1-3; sro1-1* (G, H). (I–L) Staining for GUS activity of *CYCD4;1::GUS* in the root tip: (I, K) 2 h staining and (J, L) 20 h staining; WT-like (I, J) and *rcd1-3; sro1-1* (K, L). (M–P) Staining for GUS activity of *DEL1::GUS*: (M-O), 4 h staining and (P), 20 h staining; WT-like (M, N), *rcd1-3; sro1-1* (O, P). All scale bars represent 50 μm. Scale bar in (A) applies to (A–D) and that in (E) applies to (E–P). The green lines indicate the extent of the division zone in A–D. Col-0, Columbia.

The root meristem of rcd1-3; sro1-1 *plants is small*

Consistent with the strong expression of *RCD1* and *SRO1* in the meristematic region of the root and their redundant functions, the roots of *rcd1-3; sro1-1* double mutant plants are short (Fig. 2A). This decrease in length is at least partially due to a decrease in size in the root division zone, as assayed both by length (Fig. 2B) and cell number (Fig. 2C) of the division zone.

In wild-type Arabidopsis, exit from the cell proliferation phase to the elongation phase is accompanied by entry into the endocycle (Inze and De Veylder, 2006; De Veylder *et al.*, 2007). This can be visualized by an increase in nuclear size. Consistent with a reduced division zone in *rcd1-3; sro1-1* plants, nuclear size increases closer to the tip in these plants than in wild type (Fig. 3C, D), suggesting cells exit the mitotic cycle early. The reduction in the number of cells expressing *CYCB1;1::GUS*, marking cells at the G_2–M transition (Colon-Carmona *et al.*, 1999), in *rcd1-3; sro1-1* plants also indicates a reduction in the area where division takes place in these roots (Fig. 3G, H). Disruption of expression of two other cell cycle genes, *CYCD4;1* and *E2Fe/DEL1*, also supports the idea that the normal division patterns within the root are controlled by *RCD1* and *SRO1*. *CYCD4;1* is normally expressed in a broad zone encompassing the division zone of wild-type Arabidopsis (Fig. 3I, J; De Veylder *et al.*, 1999), but is significantly reduced in double mutant roots (Fig. 3K, L). The atypical E2F factor *DEL1* is transcribed exclusively in non-endoreduplicating dividing cells (Lammens *et al.*, 2008). In *rcd1-3; sro1-1* root tips expression of this gene is barely detectable (Fig. 3O, P). However, expression of a number of other cell cycle-associated genes, although their zone of expression in double mutant roots is smaller than in wild type due to the smaller division zone, have relatively normal expression patterns (Fig. S1, Table S1).

rcd1-3; sro1-1 *plants have disorganized roots*

In addition to a reduction in cell division, *rcd1-3; sro1-1* roots are abnormally patterned and have differentiation defects. Transverse sections through the mature region of roots reveal that, unlike wild type, the xylem is harder to distinguish in double mutant roots (Fig. 4D). Xylem vessel elements are small in *rcd1-3; sro1-1* roots and their cell walls appear thinner (Fig. 4E, F). This makes differentiating between protoxylem and metaxylem difficult (Fig. 4E). The cortex, which normally consists of one layer of eight cells, contains extra cells, both around the circumference and in extra layers (Fig. 4E, F). Cell shape in the double mutant is also abnormal. This disorganization within the mature root is consistent with defects seen in the division zone of the roots. When the architecture of root tips of *rcd1-3; sro1-1* plants was examined, no clear QC can be observed (Fig. 5D–F), even as early as 2 days after germination. It is more difficult to trace cell files to initial cells in the double mutant, as division planes are abnormal in the tip region. This misplacement of division planes continues into more proximal regions of the division zone (e.g. Fig. 5D). The root cap of the double mutant is less ordered than in wild type or single *rcd1-3* or *sro1-1* mutants (Fig. 5I–K). The lateral root cap cells do not detach readily, creating a longer root cap in the majority of roots (Table 1). Examination of starch distribution within double mutant root caps demonstrates that the width of the columella is

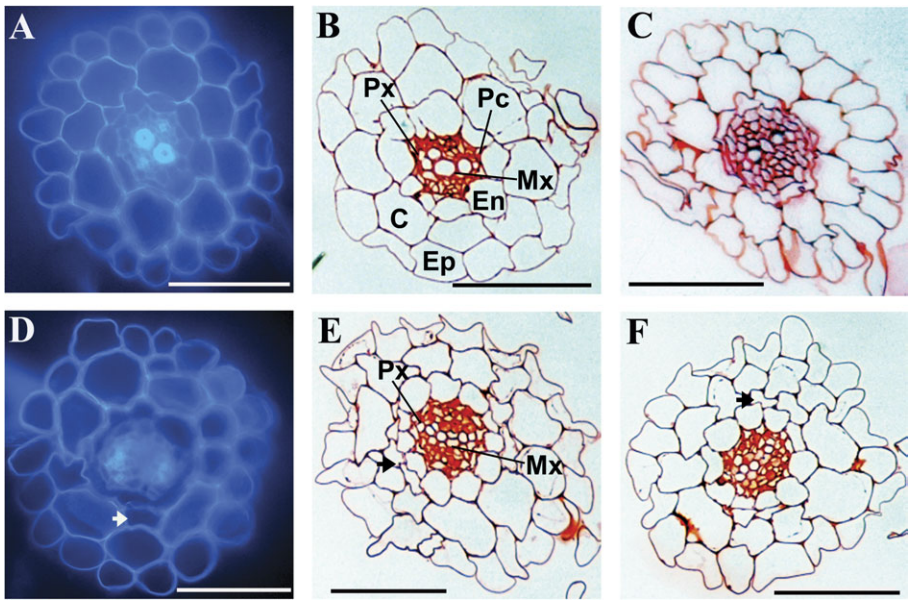

Fig. 4. *rcd1-3; sro1-1* roots have abnormal radial patterning. Transverse sections of roots within the maturation zone of wild type (A–C) and *rcd1-3; sro1-1* (D–F). (A) and (D) are hand-sections while (B, C, E, F) are thin sections. Small arrows indicate abnormal planes of cell division. All scale bars indicate 50 μm. C, cortex; En, endodermis; Ep, epidermis; Mx, metaxylem; Pc, pericycle; Px, protoxylem.

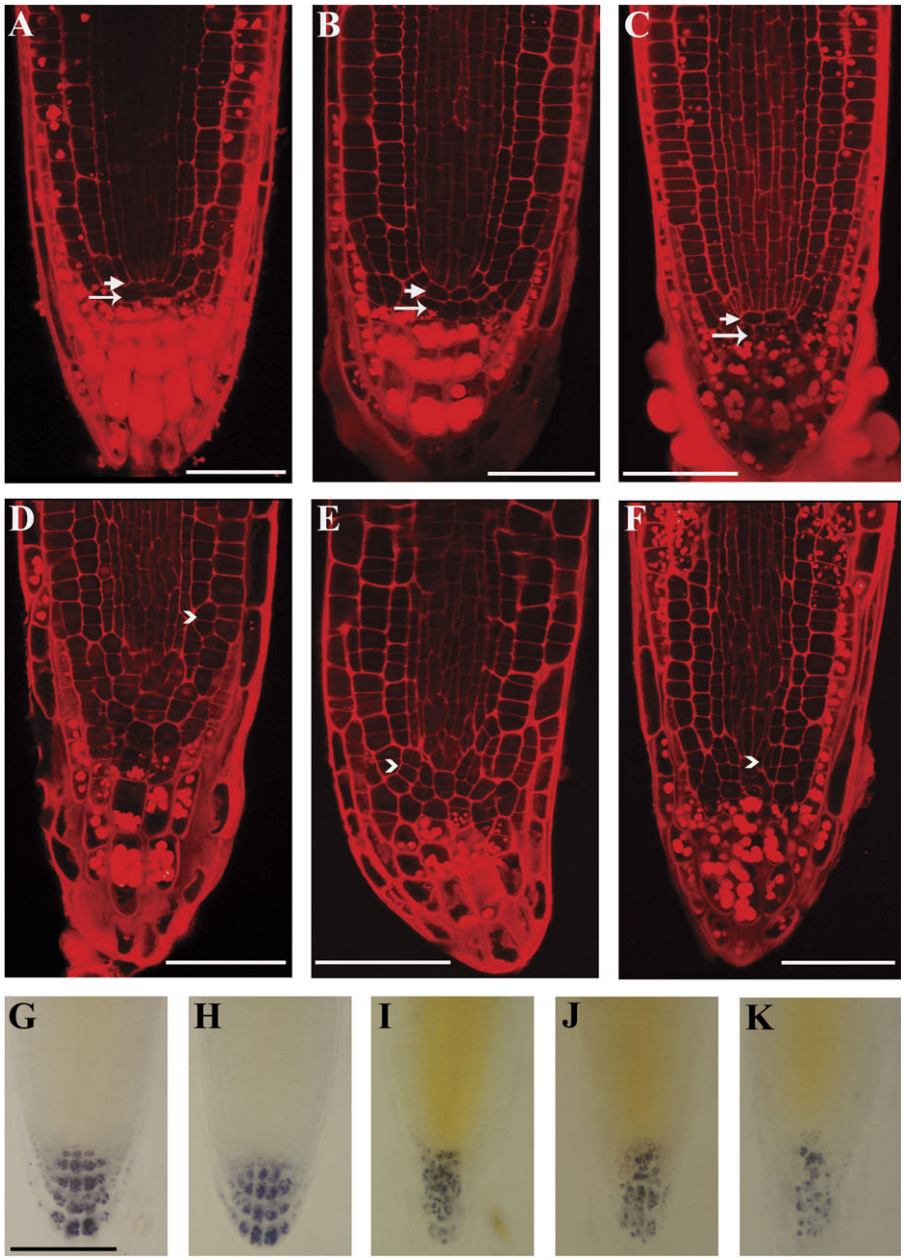

Fig. 5. *rcd1-3; sro1-1* roots have abnormal division patterns and disorganized root caps. (A–F) Root tip structure, visualized by confocal laser scanning microscopy after cell wall staining with propidium iodide: Col-0 (A), *rcd1-3* (B), *sro1-1* (C) and *rcd1-3; sro1-1* (D–F). Small arrows indicate QC, large arrows indicate columella stem cells, and arrowheads indicate abnormal planes of cell division. (G–K) Columella structure in 5-day-old seedlings: Col-0 (G, H) and *rcd1-3; sro1-1* (I–K). Scale bars in (A–F) indicate 50 μm. Scale bar in (G) represent 100 μm and applies to (G–K).

reduced, its cell layers indistinct, and the amyloplasts smaller (Fig. 5I–K), suggesting a differentiation defect in these cells.

In order to examine cell identity in the root more closely, the expression of a series of marker lines was examined in *rcd1-3; sro1-1* plants and their WT-like siblings. The expression patterns of most markers of positional identity within the root did not differ significantly between the double mutant and wild type (Fig. 6), consistent with the fact that most cell types can be distinguished in mature roots. Expression of both *PLETHORA1* and *PLETHORA2* (*PLT1*, *2*) is normal in the region of the presumed RAM in

Table 1. Lateral root cap cells are retained in *rcd1-3; sro1-1* plants

Genotype	*N*[a]	Number of roots with retained lateral root cap cells[b]
Col-0	25	2
rcd1-3; sro1-1	47	43

[a] Number of plants examined.
[b] Defined as roots in which lateral root caps are still attached to the root epidermis at least five cell lengths into the elongation zone of the primary root.

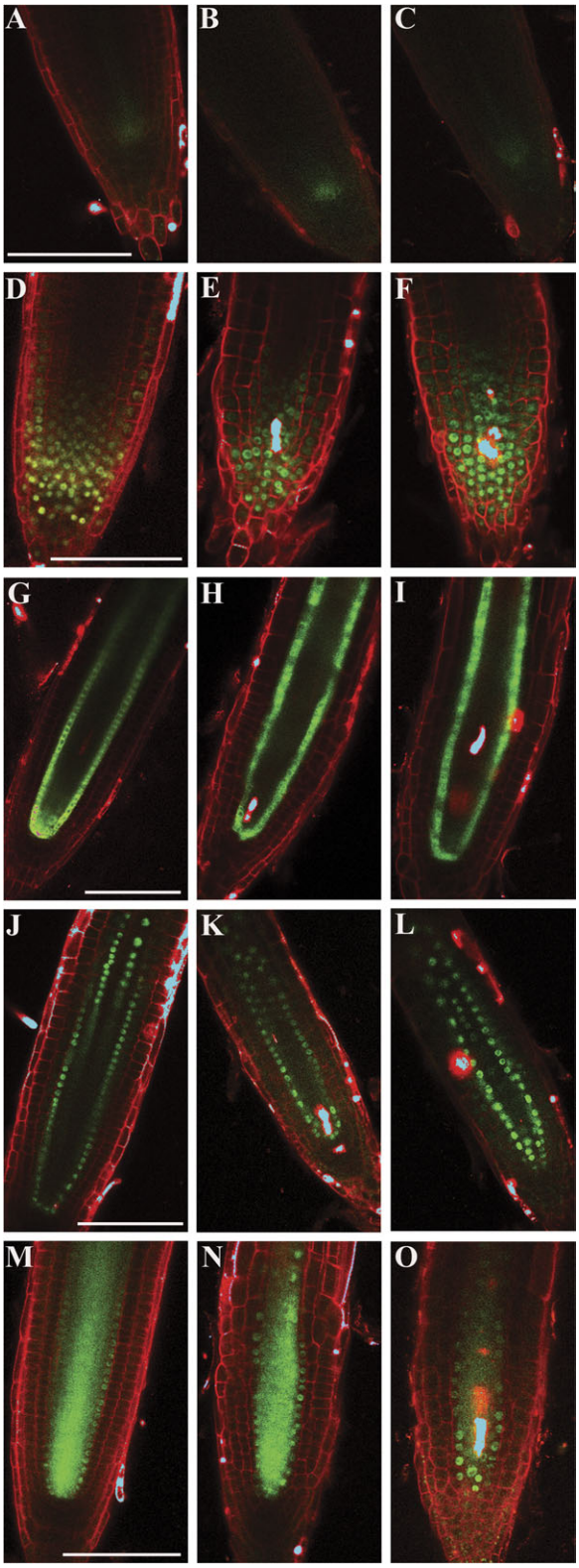

Fig. 6. Cell fate in the root tip of *rcd1-3; sro1-1* plants resemble that of wild type. Wild type-like roots (A, D, G, J, M); *rcd1-3; sro1-1* roots (B, C, E, F, H, I, K, L, N, O). *PLT1p::GFP* (A-C), *PLT2p::PLT2-GFP* (D-F), *SCRp::GFP* (G-I), *SCRp::SCR-GFP* (J-L), *SHRp::SHR-GFP* (M-O). Scale bars represent 100 μm and scale bar in each row applies to all images in that row.

rcd1-3; sro1-1 roots (Fig. 6A–F). The cell fate markers *SCARECROW* (*SCR*) and *SHORTROOT* (*SHR*) are expressed in the endodermis and stele, as in wild type (Fig. 6G–O). These results suggest that proper cell fate is acquired in mutant roots. In line with this finding, expression of many markers of auxin transport and signalling remained relatively normal in double mutant roots. Analysis of *DR5rev::GFP* (Friml *et al.*, 2003) expression in *rcd1-3; sro1-1* plants reveals that auxin maxima at the root pole and tips of forming cotyledons form in mutant embryos (Fig. 7A–H). An auxin maximum is also found at the tips of post-embryonic roots in the double mutant plants, although it is not as straight as in the wild type (Fig. 7J, K). Consistent with the presence of an auxin maximum, the expression pattern and protein localization of many components of the auxin transport system are similar to those of wild type. The auxin efflux carrier PIN1 (Benkova *et al.*, 2003) is expressed at normal levels and the protein is properly polarized in the stele of *rcd1-3; sro1-1* roots, although expression outside of the stele may be lower (Fig. 7M, N). Expression of the influx carriers AUX1 (Bennett *et al.*, 1996) and LAX3 (Swarup *et al.*, 2008), and the efflux carriers PIN2 (Muller *et al.*, 1998) and PIN4 (Friml *et al.*, 2002) are also normal (Fig. S2). AXR4, an accessory protein necessary for proper localization of AUX1 and PIN proteins (Dharmasiri *et al.*, 2006), is also correctly localized (Fig. S2). In contrast, expression of *PIN7*, as assayed by both translational (Fig. 7P, Q) and transcriptional (Fig. 7S, T) gene fusions, was abnormal in *rcd1-3; sro1-1* plants. PIN7 is normally found expressed in the stele, where the protein is localized to the basal end of the cells, and in the columella, where the protein has an apolar localization. There is a small gap in expression at the RAM (Vieten *et al.*, 2007). In *rcd1-3; sro1-1* roots, the gap in gene expression is larger than in wild type (Fig. 7S, T), although the RAM in these plants appears to be smaller. Translational fusions reveal that protein accumulation is inconsistent in the stele and appears less polarized (Fig. 7P). Some mutant roots have lost lower stele accumulation of PIN7 protein altogether (Fig. 7Q). PIN7 accumulates in columella cells of *rcd1-3; sro1-1* roots in an apolar manner as in wild type; however, the protein level appears to be higher. The number of cells expressing PIN7 in the columella is fewer and those cells are abnormally shaped (Fig. 7P, Q). In order to determine whether the *rcd1-3; sro1-1* plants respond normally to auxin and to cytokinin, which regulates auxin efflux and biosynthesis (Pernisova *et al.*, 2009; Jones *et al.*, 2010), the effect of exogenously applied hormones on the mutants was examined. Both *rcd1-3* and *sro1-1* single mutants and the double mutant are able to respond to exogenously applied NAA (Table S2) and BA (Table S3). The *rcd1-3; sro1-1* plants may be slightly hypersensitive to both hormones, but this is inconclusive due to the limited growth of double mutant roots. Overall, it appears that the double mutant plants have relatively normal auxin and cytokinin responses.

Although many markers of cell fate have near wild-type expression patterns in *rcd1-3; sro1-1* roots, the expression of

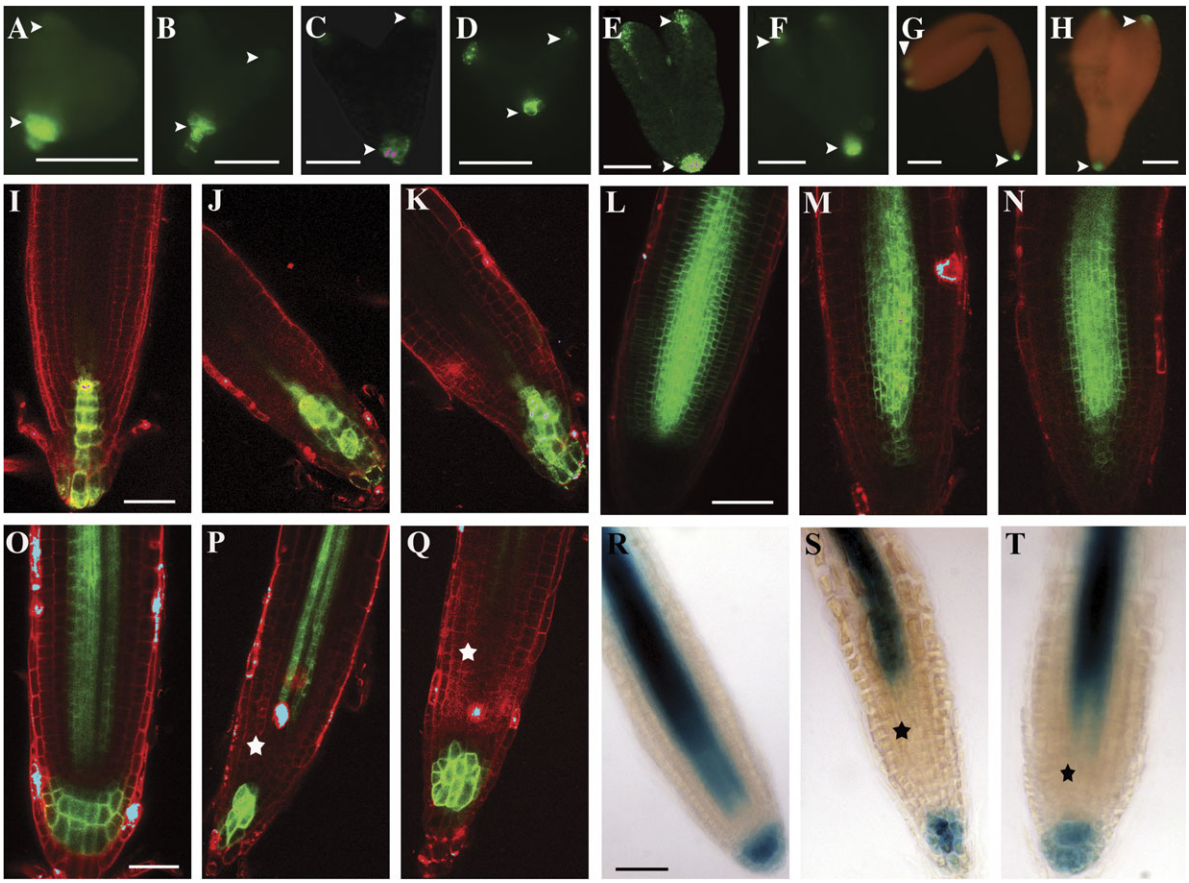

Fig. 7. Auxin transport proteins accumulate normally in *rcd1-3; sro1-1* embryos and roots. Wild type (A, C, E, G, I); wild type-like (L, O, R); *rcd1-3; sro1-1* (B, D, F, H, J, K, M, N, P, Q, S, T). *DR5rev::GFP* (A-K), *PIN1p::PIN1-GFP* (L-N), *PIN7p::PIN7-GFP* (O-Q), *PIN7p::GUS* (R-T). The arrowheads in (A-H) indicate auxin maxima through *DR5rev::GFP* expression while the stars in (P, Q) mark gaps in PIN7 protein accumulation. All scale bars represent 100 μm and bars in (I, L, O, R) apply to the corresponding double mutant images for the respective marker line.

QC markers was considerably reduced (Fig. 8A–J), consistent with a lack of morphologically identifiable QC cells. Under relatively short staining times, when WT-like roots show strong staining of both QC184 and QC25 (Fig. 8A, F), *rcd1-3; sro1-1* roots had no detectable staining (Fig. 8B, G). After longer staining times, some double mutant roots showed faint QC184 expression in what appears to be root cap cells and some expression of QC25 in what appears to be a single cell that is displaced towards the distal end of the root (Fig. 8D, E, I, J). This suggests that QC identity is compromised in *rcd1-3; sro1-1* roots.

The defects seen in the mature region of the *rcd1-3; sro1-1* roots suggest that cell differentiation outside of the QC may be disrupted. This is supported by misexpression of at least one marker line within the root. The GRAS family transcription factor *SCARECROW-LIKE3* (*SCL3*) is normally expressed in the endodermis (Fig. 8L; Pysh *et al.*, 1999). In double mutant roots, expression of this gene is expanded into other cell layers of the root, including the cortex and lateral root cap cells (Fig. 8M, N). Although the function of *SCL3* is not known, this misexpression suggests problems with transcriptional control in the outer layers of the *rcd1-3; sro1-1* roots.

Cell division and differentiation are defective in the above-ground portion of rcd1-3; sro1-1 *plants*

rcd1-3; sro1-1 adult plants are short with small leaves and flowers (Jaspers *et al.*, 2009; Teotia and Lamb, 2009), suggesting that cell proliferation may be defective in these areas of the plant as well. Consistent with this, the leaves and stems of double mutant plants are smaller with fewer cells (Fig. 9C, G, K). Patterning and differentiation is also disrupted in these organs. Transverse sections of leaves reveal that *rcd1-3; sro1-1* leaves have a disorganized palisade parenchyma layer containing misshapen cells and large gaps (Fig. 9C). The cuticle of the epidermis appears thinner, suggesting either that there is less cuticle secreted or that the chemical composition of the cuticle has changed. The leaf vascular bundles have poorly differentiated xylem and xylem fibres are either missing or have not made extensive secondary cell wall (Fig. 9D).

Stems in *rcd1-3; sro1-1* plants are significantly reduced in diameter (Fig. 9G, K). Examination of cell patterning and differentiation at the base of the inflorescence stem demonstrates that there is a reduced pith region in the centre of the stem, abnormal cuticle secreted by the epidermis, and oddly

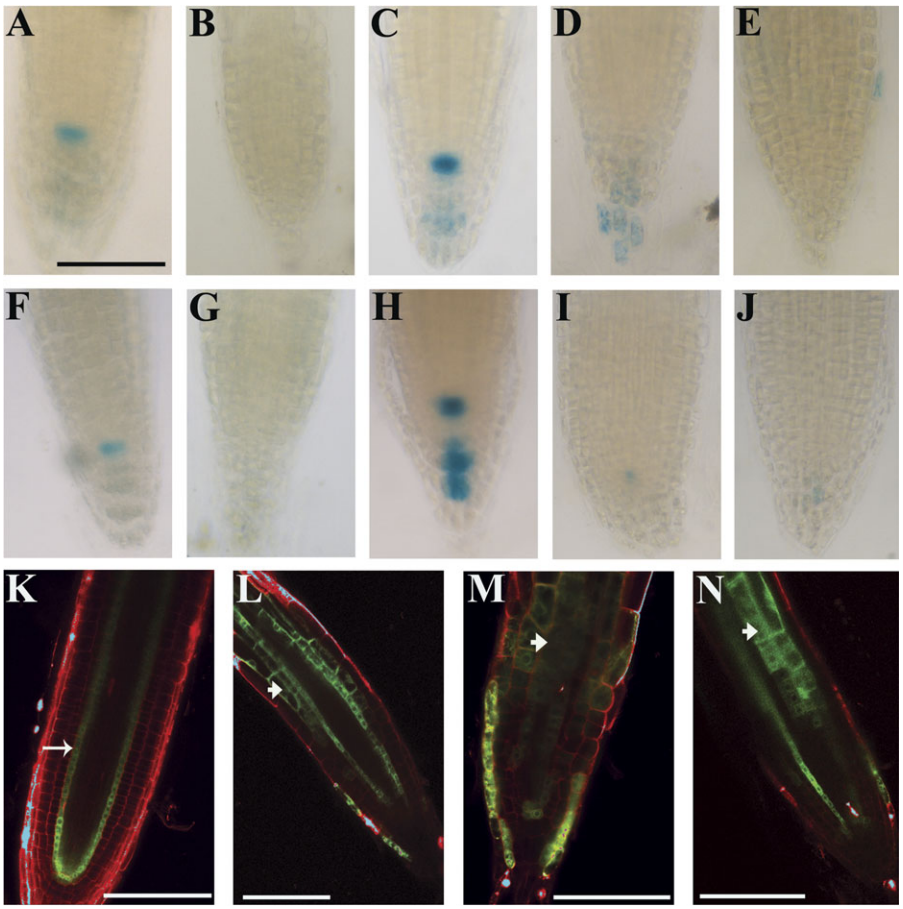

Fig. 8. RCD1 and SRO1 control cell identity within the QC. Staining for GUS activity in the QC marker lines QC184 (A–E) and QC25 (F–J): 2 h of staining (A, B, F, G), 20 h of staining (C, D, E, H, I, J), WT-like (A, C, F, H), *rcd1-3; sro1-1* (B, D, E, G, I, J). (K-N) Expression of *SCL3p::GFP* in the root visualized by confocal laser scanning microscopy after cell wall staining with propidium iodide: Wild type-like (K), *rcd1-3; sro1-1* (L-N). Large arrow indicates the endodermis while small arrows indicate other cell layers. All scale bars represent 100μm. Scale bar in (A) applies to (A-J).

shaped cortical cells (Fig. 9G, H). The vascular cambium is interrupted by gaps and there are areas in the stem where secondary phloem has been produced, but the corresponding secondary xylem has either failed to differentiate or was not produced by the cambium (Fig. 9H). Metaxylem can be seen located close to the cambium, suggesting that the secondary xylem was not formed. The region of the stem nearer the inflorescence meristem has reduced pith and expanded cortex (Fig. 9K). The vascular bundles are fewer in number than wild type but contain both phloem and xylem, although it is difficult to distinguish protoxylem from metaxylem (Fig. 9L). Fascicular vascular cambium appears to be missing from some individual vascular bundles although it can be distinguished in others. In general, the defects seen in both leaves and stems of *rcd1-3; sro1-1* plants are consistent with defects in division, differentiation and maintenance of meristematic stem populations. However, most cell types are present.

The reduced cell division in roots, leaves and stems and the disappearance of the QC of the roots and vascular cambium of the stem suggests that meristematic cell fate maintenance needs functional *RCD1* and *SRO1*. Flower production on the primary inflorescence of *rcd1-3; sro1-1* plants and wild type was examined as a proxy for inflorescence meristem function. The number of flowers produced by double mutant plants is significantly reduced compared with wild type (Table 2), suggesting that this meristem may fail to be maintained.

Discussion

The PARP superfamily is found across the eukaryotes (Citarelli *et al.*, 2010). *RCD1* and *SRO1* encode partially redundant members of a land-plant-specific clade of PARP-like proteins that localize to the nucleus. In this work, we demonstrate that these genes function to control division and differentiation in the root. They are necessary to maintain QC identity within the RAM and to support the population of dividing cells of this region; subsequently they are required for proper differentiation, both at an organ level and at an individual cell level.

The requirement for *RCD1* and *SRO1* in maintaining cells in a division-competent state is supported by several lines of evidence. Roots of *rcd1-3; sro1-1* plants grow slowly

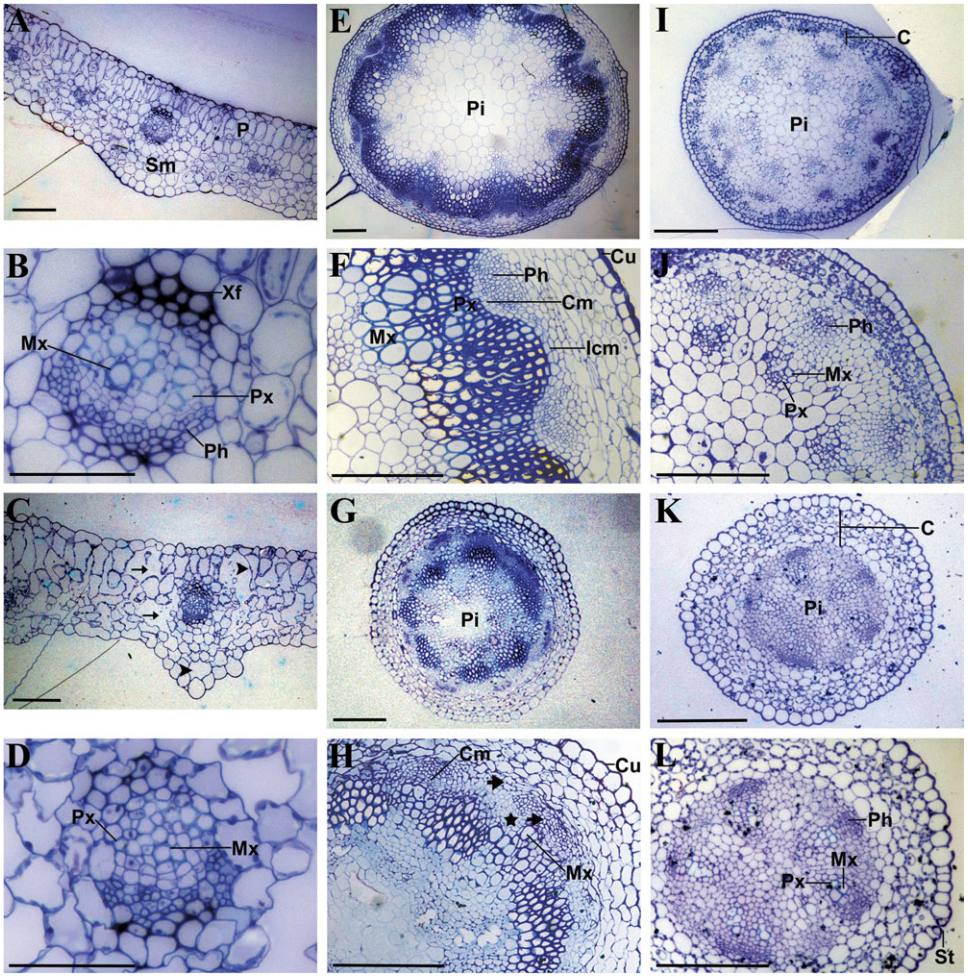

Fig. 9. Cell division, patterning and differentiation are defective in the aerial organs of *rcd1-3; sro1-1* plants. Col-0 (A, B, E, F, I, J) and *rcd1-3; sro1-1* (C, D, G, H, K, L). (A–D) Transverse sections of leaves stained with toluidine blue: arrowheads indicate misshapen cells and arrows indicate large intercellular gaps. (E–H) Transverse sections of stems stained with toluidine blue, through the base of the inflorescence stem. Small arrows indicate gaps in the vascular cambium while stars indicate interruptions in the continuity of secondary growth. (I–L) Transverse sections of stems stained with toluidine blue, through the apical region. Scale bars in (B) and (D) represent 50 μm, all other scale bars represent 100 μm. Col-0, Columbia; C, cortex; Cm, cambium; Cu, cuticle; Icm, interfascicular cambium; Mx, metaxylem; P, palisade cells; Ph, phloem; Pi, pith; Px, protoxylem; Sm, spongy mesophyll; St, stomata; Xf, xylem fibres.

Table 2. *rcd1-3; sro1-1* plants make few flowers

Genotype	N[a]	Average number of flowers[b]	Standard deviation
Col-0	25	55.6	11.0
rcd1-3; sro1-1	25	16.6[c]	3.1

[a] Number of plants.
[b] Primary inflorescence only.
[c] Significantly different from Col-0 at $P < 0.001$.

to a shorter length and this correlates with fewer cells in the division zone (Fig. 2). Cells in the *rcd1-3; sro1-1* root tip begin endoreduplicating their DNA close to the tip, suggesting that they have exited mitotic division. This morphological observation is supported by the fact that a smaller population of cells in the tip region of the double mutant express the division marker *CYCB1;1* (Fig. 3; Colon-Carmona *et al.*, 1999). The expression of two other cell cycle-related genes in *rcd1-3; sro1-1* root tips, *CYCD4;1* (Barroco *et al.*, 2005) and *DEL1* (Lammens *et al.*, 2008), is almost undetectable (Fig. 3K, L, O, P), supporting the interpretation that mitotic cell division at the root tip is reduced. There does not appear to be a general problem with the cell cycle in *rcd1-3; sro1-1* mutants, since the majority of cell cycle genes are expressed normally (Fig. S1). A reduction in cell division can also be inferred in the aerial portions of *rcd1-3; sro1-1* plants. Both leaves and stems of the double mutant are smaller with fewer cells (Fig. 9). More importantly, the vascular cambium is disrupted in the stem of these plants; it appears that cells of the cambium have exited the cell cycle and differentiated, leading to a reduction in secondary growth. Differentiation of many cell types is abnormal in *rcd1-3; sro1-1* leaves and stems (Fig. 9). Interestingly, the cuticle secreted by leaf epidermal cells appears thinner, due to either a change in composition

or a reduction in amount (Fig. 9C, D). Neither *RCD1* nor *SRO1* is expressed in pavement cells of the leaf epidermis (although they are expressed in guard cells (Winter *et al.*, 2007; Jaspers *et al.*, 2009) suggesting that any change in cuticle production by those cells is a non-autonomous function of these genes.

Our results indicate that *RCD1* and *SRO1* are necessary for proper organization of the RAM and the distal root. In *rcd1-3; sro1-1* mutants QC cells cannot be histologically identified (Fig. 5) and expression of two different QC markers is disrupted (Fig. 8), suggesting that QC cells have lost at least some of their proper identity. The QC is necessary to sustain root meristem function and indeterminate growth of the root, which appears to be compromised in the mutants. The fate of the QC and surrounding cells is established by the actions of auxin and the *PLT* genes. An auxin gradient with a maximum near the tip is generated by flux of this hormone and this is sufficient to form meristematic and elongation zones (Grieneisen *et al.*, 2007). Auxin induces the expression of the *PLT* genes (Aida *et al.*, 2004), which in turn regulate auxin transport as the triple mutant *plt1; 2 ; 3* shows reduced or no expression of *PIN1, PIN2*, and *PIN3* (Galinha *et al.*, 2007), demonstrating that these two pathways are interdependent. Once the meristem has been established, *WUSCHEL-RELATED HOMEOBOX 5* (*WOX5*), *SHR*, and *SCR* transcription factors control the activities and identity of those cells (Sabatini *et al.*, 1999, 2003; Stahl *et al.*, 2009). In order to determine whether disruption of any of these pathways contributes to the root meristem defects we see in *rcd1-3; sro1-1* plants, we examined the expression of *PLT1*, *PLT2*, *SHR*, and *SCR* in this background (Fig. 6). The expression of these genes was similar to the wild type, suggesting that cell fate in the region is established normally and that the maintenance of the meristem and identity of QC cells is affected in *rcd1-3; sro1-1* by pathways at least partially independent of the above-mentioned genes.

Auxin homeostasis appears to be relatively normal in *rcd1-3; sro1-1* plants as well. Auxin maxima form in the embryo and are maintained in the post-embryonic root, based on expression of *DR5rev::GFP* (Fig. 7). Expression of the auxin efflux carriers *PIN1*, *PIN2*, and *PIN4*, and the influx carriers *AUX1* and *LAX3* did not significantly change in the *rcd1-3; sro1-1* mutants (Figs 7, S2). However, expression and accumulation of PIN7 were disrupted, with a larger gap between stele and columella zones or complete absence in the stele, accompanied by increased expression in fewer cells of the columella. The disruption in root cap organization and maturation we observed might be at least partially caused by the higher levels of PIN7 accumulation in the root tip, leading to a depletion of auxin signalling in the cap and subsequent patterning and differentiation abnormalities in the root cap, although this remains to be investigated.

In addition to the pathways discussed above, QC identity and activity are regulated by redox balance. Glutathione (GSH) has been localized to the meristem and the hair cell files within the epidermis in Arabidopsis roots; however, it was not seen within the QC cells (Sanchez-Fernandez *et al.*, 1997). This suggests that QC cells may accumulate more oxidants than surrounding cells. In maize, this is known to be true (Jiang *et al.*, 2003) and it has been demonstrated that altering this can affect meristem function (Sanchez-Fernandez *et al.*, 1997; Kerk *et al.*, 2000). Loss of the GSH biosynthetic enzyme encoded by *ROOT MERISTEMLESS1* (*RML1*) causes loss of the root meristem and no post-embryonic root, suggesting that GSH is essential for root meristem maintenance (Vernoux *et al.*, 2000). Recent work has demonstrated that GSH is necessary for QC identity and auxin maxima formation by, directly or indirectly, stabilizing accumulation of the auxin efflux carriers PIN1, PIN2, and PIN7 (Koprivova *et al.*, 2010). *rcd1* mutants are known to accumulate ROS and reactive nitrogen species (Overmyer *et al.*, 2000; Ahlfors *et al.*, 2008) and upregulate genes involved in oxidative stress response (Jaspers *et al.*, 2009). *rcd1-3; sro1-1* double mutants appear to be under constitutive stress and their phenotypes resemble those of SIMR (Teotia *et al.*, 2010). Typical SIMR responses include decreases in root length, stem height, and leaf area, altered xylem development, and redistribution of cell division and elongation (reviewed by Potters *et al.*, 2009). Importantly, the primary RAM stops dividing during SIMR, leading to shorter roots and disorganized meristems. Therefore, we hypothesize that the meristem defects we see in *rcd1-3; sro1-1* plants may be due to a SIMR-like phenomenon, and that a primary function of RCD1 and SRO1 is to control, directly or indirectly, redox balance in the cell. Since RCD1 and SRO1 have been shown to bind, at least in yeast two-hybrid experiments, to a variety of transcription factors (Belles-Boix *et al.*, 2000; Ahlfors *et al.*, 2004; Jaspers *et al.*, 2010), it may control the redox environment by impacting functions of these proteins.

Supplementary material

Supplementary Fig. S1. The cell cycle is not generally disrupted in *rcd1-3; sro1-1* plants. Wild type-like (A, C, E, G, I, K, M, O, Q, S, U) and *rcd1-3; sro1-1* (B, D, F, H, J, L, N, P, R, T, V). *CDKA;1p::GUS* (A, B); *CDKB1;1p::GUS* (C, D); *CYCA2;3p::GUS* (E, F); *CDKD;1p::GUS* (G, H); *CYCA2;1p::GUS* (I, J); *E2fap::GUS* (K, L); *CKS1p::GUS* (M, N); *CYCD3;1p::GUS* (O, P); *DEL3p::GUS* (Q, R); *KRP2p::GUS* (S, T); *WEE1p::GUS* (U, V). Scale bars in (A–L) represent 50 μm, while scale bars in (M-V) represent 1 mm. For each marker line, a scale bar is shown in the wild type-like image that also applies to the corresponding double mutant image.

Supplementary Fig. S2. Expression of auxin transport components is normal in *rcd1-3; sro1-1* plants. Wild type-like (A, C, E, G, I) and *rcd1-3; sro1-1* (B, D, F, H, J). *PIN2p::PIN2-GFP* (A, B); *PIN4p::PIN4-GFP* (C, D); *AXR4p::AXR4-YFP* (E, F); *AUX1p::AUX1-GFP* (G, H); *LAX3p::LAX3-YFP* (I, J). Scale bars represent 50 μm and scale bar in each row applies to both images in that row.

Supplementary Table S1. Transgenic lines used in this study.

Supplementary Table S2. Auxin sensitivity.
Supplementary Table S3. Cytokinin sensitivity.

Acknowledgements

We thank Dr Takashi Aoyama (Kyoto University), Dr Philip Benfey (Duke University), Dr Malcolm Bennett (University of Nottingham), Dr Thomas Berleth (University of Toronto), Dr Steven Clark (University of Michigan), Dr Lieven De Veylder (Ghent University), Dr Peter Doerner (University of Edinburgh), Dr Jiri Friml (Ghent University), Dr Jaakko Kangasjarvi (University of Helsinki), and Dr Ben Scheres (University of Utrecht) for sharing marker lines. We also thank the Arabidopsis Biological Resource Center and the European Arabidopsis Stock Centre for seeds. We further thank Dr Tea Meulia and the Molecular and Cellular Imaging Center, Ohio Agricultural Research and Development Center, The Ohio State University for assistance with histology and microscopy, Mr Zachary Skidmore (The Ohio State University) for technical assistance and Dr Iris Meier (The Ohio State University) for reading of the manuscript. Funding for this work was supplied by The Ohio State University and the Citarelli Fund.

References

Adams-Phillips L, Briggs AG, Bent AF. 2010. Disruption of poly(ADP-ribosyl)ation mechanisms alters responses of Arabidopsis to biotic stress. *Plant Physiology* **152,** 267–280.

Adams-Phillips L, Wan J, Tan X, Dunning FM, Meyers BC, Michelmore RW, Bent AF. 2008. Discovery of ADP-ribosylation and other plant defense pathway elements through expression profiling of four different Arabidopsis-Pseudomonas R-avr interactions. *Molecular Plant–Microbe Interactions* **21,** 646–657.

Ahlfors R, Brosché M, Kollist H, Kangasjärvi J. 2008. Nitric oxide modulates ozone-induced cell death, hormone biosynthesis and gene expression in *Arabidopsis thaliana*. *The Plant Journal* Nov 28 [Epub ahead of print].

Ahlfors R, Lang S, Overmyer K, *et al*. 2004. Arabidopsis RADICAL-INDUCED CELL DEATH1 belongs to the WWE protein-protein interaction domain protein family and modulates abscisic acid, ethylene, and methyl jasmonate responses. *The Plant Cell* **16,** 1925–1937.

Aida M, Beis D, Heidstra R, Willemsen V, Blilou I, Galinha C, Nussaume L, Noh YS, Amasino R, Scheres B. 2004. The *PLETHORA* genes mediate patterning of the Arabidopsis root stem cell niche. *Cell* **119,** 109–120.

Amor Y, Babiychuk E, Inze D, Levine A. 1998. The involvement of poly(ADP-ribose) polymerase in the oxidative stress responses in plants. *FEBS Letters* **440,** 1–7.

Babiychuk E, Cottrill PB, Storozhenko S, Fuangthong M, Chen Y, O'Farrell MK, Van Montagu M, Inze D, Kushnir S. 1998. Higher plants possess two structurally different poly(ADP-ribose) polymerases. *The Plant Journal* **15,** 635–645.

Barroco RM, Van Poucke K, Bergervoet JH, De Veylder L, Groot SP, Inze D, Engler G. 2005. The role of the cell cycle machinery in resumption of postembryonic development. *Plant Physiology* **137,** 127–140.

Belles-Boix E, Babiychuk E, Van Montagu M, Inze D, Kushnir S. 2000. CEO1, a new protein from *Arabidopsis thaliana*, protects yeast against oxidative damage. *FEBS Letters* **482,** 19–24.

Benfey PN, Linstead PJ, Roberts K, Schiefelbein JW, Hauser MT, Aeschbacher RA. 1993. Root development in Arabidopsis: four mutants with dramatically altered root morphogenesis. *Development* **119,** 57–70.

Benkova E, Michniewicz M, Sauer M, Teichmann T, Seifertova D, Jurgens G, Friml J. 2003. Local, efflux-dependent auxin gradients as a common module for plant organ formation. *Cell* **115,** 591–602.

Bennett MJ, Marchant A, Green HG, May ST, Ward SP, Millner PA, Walker AR, Schulz B, Feldmann KA. 1996. Arabidopsis *AUX1* gene: a permease-like regulator of root gravitropism. *Science* **273,** 948–950.

Citarelli M, Teotia S, Lamb RS. 2010. Evolutionary history of the poly(ADP-ribose) polymerase gene family in eukaryotes. *BMC Evolutionary Biology* **10,** 308.

Colon-Carmona A, You R, Haimovitch-Gal T, Doerner P. 1999. Technical advance: spatio-temporal analysis of mitotic activity with a labile cyclin-GUS fusion protein. *The Plant Journal* **20,** 503–508.

De Block M, Verduyn C, De Brouwer D, Cornelissen M. 2005. Poly(ADP-ribose) polymerase in plants affects energy homeostasis, cell death and stress tolerance. *The Plant Journal* **41,** 95–106.

De Tullio MC, Jiang K, Feldman LJ. 2010. Redox regulation of root apical meristem organization: connecting root development to its environment. *Plant Physiology and Biochemistry* **48,** 328–336.

De Veylder L, Beeckman T, Inze D. 2007. The ins and outs of the plant cell cycle. *Nature Reviews Molecular Cell Biology* **8,** 655–665.

De Veylder L, de Almeida Engler J, Burssens S, Manevski A, Lescure B, Van Montagu M, Engler G, Inze D. 1999. A new D-type cyclin of Arabidopsis thaliana expressed during lateral root primordia formation. *Planta* **208,** 453–462.

Dharmasiri S, Swarup R, Mockaitis K, *et al*. 2006. AXR4 is required for localization of the auxin influx facilitator AUX1. *Science* **312,** 1218–1220.

Doucet-Chabeaud G, Godon C, Brutesco C, de Murcia G, Kazmaier M. 2001. Ionising radiation induces the expression of *PARP-1* and *PARP-2* genes in Arabidopsis. *Molecular Genetics and Genomics* **265,** 954–963.

Foyer CH, Pellny TK, Locato V, De Gara L. 2008. Analysis of redox relationships in the plant cell cycle: determinations of ascorbate, glutathione and poly(ADPribose) polymerase (PARP) in plant cell cultures. *Methods in Molecular Biology* **476,** 199–215.

Friml J, Benkova E, Blilou I, *et al*. 2002. AtPIN4 mediates sink-driven auxin gradients and root patterning in Arabidopsis. *Cell* **108,** 661–673.

Friml J, Vieten A, Sauer M, Weijers D, Schwarz H, Hamann T, Offringa R, Jurgens G. 2003. Efflux-dependent auxin gradients establish the apical-basal axis of Arabidopsis. *Nature* **426,** 147–153.

Grieneisen VA, Xu J, Maree AF, Hogeweg P, Scheres B. 2007. Auxin transport is sufficient to generate a maximum and gradient guiding root growth. *Nature* **449,** 1008–1013.

Galinha C, Hofhuis H, Luijten M, Willemsen V, Blilou I, Heidstra R, Scheres B. 2007. PLETHORA proteins as dose-dependent master regulators of Arabidopsis root development. *Nature* **449,** 1053–1057.

Hassa PO, Hottiger MO. 2008. The diverse biological roles of mammalian PARPS, a small but powerful family of poly-ADP-ribose polymerases. *Frontiers in Bioscience* **13,** 3046–3082.

Hottiger MO, Hassa PO, Luscher B, Schuler H, Koch-Nolte F. 2010. Toward a unified nomenclature for mammalian ADP-ribosyl transferases. *Trends in Biochemical Sciences* **35,** 208–219.

Inze D, De Veylder L. 2006. Cell cycle regulation in plant development. *Annual Review of Genetics* **40,** 77–105.

Jaspers P, Blomster T, Brosche M, *et al*. 2009. Unequally redundant *RCD1* and *SRO1* mediate stress and developmental responses and interact with transcription factors. *The Plant Journal* .

Jaspers P, Overmyer K, Wrzaczek M, Vainonen JP, Blomster T, Salojarvi J, Reddy RA, Kangasjarvi J. 2010. The RST and PARP-like domain containing SRO protein family: analysis of protein structure, function and conservation in land plants. *BMC Genomics* **11,** 170.

Jiang K, Meng YL, Feldman LJ. 2003. Quiescent center formation in maize roots is associated with an auxin-regulated oxidizing environment. *Development* **130,** 1429–1438.

Jones B, Gunnerås SA, Petersson SV, Tarkowski P, Graham N, May S, Dolezal K, Sandberg G, Ljung K. 2010. Cytokinin regulation of auxin synthesis in arabidopsis involves a homeostatic feedback loop regulated via auxin and cytokinin signal transduction. *The Plant Cell* Sep 7 [Epub ahead of print].

Kerk NM, Jiang K, Feldman LJ. 2000. Auxin metabolism in the root apical meristem. *Plant Physiology* **122,** 925–932.

Koprivova A, Mugford ST, Kopriva S. 2010. Arabidopsis root growth dependence on glutathione is linked to auxin transport. *Plant Cell Reports* **29,** 1157–1167.

Lammens T, Boudolf V, Kheibarshekan L, *et al*. 2008. Atypical E2F activity restrains APC/CCCS52A2 function obligatory for endocycle onset. *Proceedings of the National Academy of Sciences, USA* **105,** 14721–14726.

Lepiniec L, Babiychuk E, Kushnir S, Van Montagu M, Inze D. 1995. Characterization of an Arabidopsis thaliana cDNA homologue to animal poly(ADP-ribose) polymerase. *FEBS Letters* **364,** 103–108.

Muller A, Guan C, Galweiler L, *et al*. 1998. *AtPIN2* defines a locus of Arabidopsis for root gravitropism control. *EMBO J* **17,** 6903–6911.

Overmyer K, Tuominen H, Kettunen R, Betz C, Langebartels C, Sandermann Jr. H, Kangasjarvi J. 2000. Ozone-sensitive Arabidopsis *rcd1* mutant reveals opposite roles for ethylene and jasmonate signaling pathways in regulating superoxide-dependent cell death. *The Plant Cell* **12,** 1849–1862.

Pellny TK, Locato V, Vivancos PD, Markovic J, De Gara L, Pallardo FV, Foyer CH. 2009. Pyridine nucleotide cycling and control of intracellular redox state in relation to poly(ADP-ribose) polymerase activity and nuclear localization of glutathione during exponential growth of Arabidopsis cells in culture. *Molecular Plant* **2,** 442–456.

Pernisova M, Klima P, Horak J, *et al*. 2009. Cytokinins modulate auxin-induced organogenesis in plants via regulation of the auxin efflux. *Proceedings of the National Academy of Sciences, USA* **106,** 3609–3614.

Potters G, Pasternak TP, Guisez Y, Jansen MA. 2009. Different stresses, similar morphogenic responses: integrating a plethora of pathways. *Plant Cell and Environment* **32,** 158–169.

Pysh LD, Wysocka-Diller JW, Camilleri C, Bouchez D, Benfey PN. 1999. The GRAS gene family in Arabidopsis: sequence characterization and basic expression analysis of the *SCARECROW-LIKE* genes. *The Plant Journal* **18,** 111–119.

Sabatini S, Beis D, Wolkenfelt H, *et al*. 1999. An auxin-dependent distal organizer of pattern and polarity in the Arabidopsis root. *Cell* **99,** 463–472.

Sabatini S, Heidstra R, Wildwater M, Scheres B. 2003. *SCARECROW* is involved in positioning the stem cell niche in the Arabidopsis root meristem. *Genes and Development* **17,** 354–358.

Sanchez-Fernandez R, Fricker M, Corben LB, White NS, Sheard N, Leaver CJ, Van Montagu M, Inze D, May MJ. 1997. Cell proliferation and hair tip growth in the Arabidopsis root are under mechanistically different forms of redox control. *Proceedings of the National Academy of Sciences, USA* **94,** 2745–2750.

Stahl Y, Wink RH, Ingram GC, Simon R. 2009. A signaling module controlling the stem cell niche in Arabidopsis root meristems. *Current Biology* **19,** 909–914.

Sugimoto K, Williamson RE, Wasteneys GO. 2000. New techniques enable comparative analysis of microtubule orientation, wall texture, and growth rate in intact roots of Arabidopsis. *Plant Physiology* **124,** 1493–1506.

Swarup K, Benkova E, Swarup R, *et al*. 2008. The auxin influx carrier LAX3 promotes lateral root emergence. *Nature Cell Biology* **10,** 946–954.

Teotia S, Lamb RS. 2009. The paralogous genes *RADICAL-INDUCED CELL DEATH1* and *SIMILAR TO RCD ONE1* have partially redundant functions during Arabidopsis development. *Plant Physiology* **151,** 180–198.

Teotia S, Muthuswamy S, Lamb RS. 2010. *RADICAL-INDUCED CELL DEATH1* and *SIMILAR TO RCD ONE1* and the stress-induced morphogenetic response. *Plant Signaling and Behavior* **5,** 143–145.

Truernit E, Bauby H, Dubreucq B, Grandjean O, Runions J, Barthelemy J, Palauqui JC. 2008. High-resolution whole-mount imaging of three-dimensional tissue organization and gene expression enables the study of phloem development and structure in Arabidopsis. *The Plant Cell* **20,** 1494–1503.

van den Berg C, Willemsen V, Hendriks G, Weisbeek P, Scheres B. 1997. Short-range control of cell differentiation in the Arabidopsis root meristem. *Nature* **390,** 287–289.

Vanderauwera S, De Block M, Van de Steene N, van de Cotte B, Metzlaff M, Van Breusegem F. 2007. Silencing of poly(ADP-ribose) polymerase in plants alters abiotic stress signal transduction. *Proceedings of the National Academy of Sciences, USA* **104,** 15150–15155.

Vernoux T, Wilson RC, Seeley KA, *et al*. 2000. The *ROOT MERISTEMLESS1/CADMIUM SENSITIVE2* gene defines a glutathione-dependent pathway involved in initiation and maintenance of cell division during postembryonic root development. *The Plant Cell* **12,** 97–110.

Vieten A, Sauer M, Brewer PB, Friml J. 2007. Molecular and cellular aspects of auxin-transport-mediated development. *Trends in Plant Science* **12,** 160–168.

Willemsen V, Wolkenfelt H, de Vrieze G, Weisbeek P, Scheres B. 1998. The *HOBBIT* gene is required for formation of the root meristem in the Arabidopsis embryo. *Development* **125,** 521–531.

Winter D, Vinegar B, Nahal H, Ammar R, Wilson GV, Provart NJ. 2007. An 'Electronic Fluorescent Pictograph' browser for exploring and analyzing large-scale biological data sets. *PLoS One* 2, e718.